

# The role of spike-timing-dependent plasticity and random inputs in neurodegenerative diseases and neuromorphic systems

Thoa Thieu<sup>1</sup> and Roderick Melnik<sup>2,3</sup>

<sup>1</sup> School of Mathematical and Statistical Sciences, The university of Texas Rio Grande Valley  
Edinburg, Texas, USA

<sup>2</sup> MS2Discovery Interdisciplinary Research Institute, Wilfrid Laurier University,  
75 University Ave W, Waterloo, Ontario, Canada N2L 3C5

<sup>3</sup> BCAM - Basque Center for Applied Mathematics, Bilbao, Spain  
thoa.thieu@utrgv.edu, rmelnik@wlu.ca

**Abstract.** Neuronal oscillations are related to symptoms of Parkinson’s disease. The random inputs could affect such oscillations in the brain states that translate collective activities of neurons interconnected via synaptic connections. In this paper, we study coupled effects of channels and synaptic dynamics under the stochastic influence, together with spike-timing-dependent plasticity (STDP) of healthy brain cells with applications to Parkinson’s disease (PD). In particular, we investigate the effects of random inputs and input correlations in a subthalamic nucleus (STN) cell membrane potential model. Our numerical results show that the random inputs strongly affect the spiking activities of the STN neuron not only in the case of healthy cells but also in the case of PD cells in the presence of DBS treatment. The STDP increases the interspike interval (ISI) regularity of spike trains of the output neurons. However, the existence of a random refractory period and random input current in the system may substantially influence an increased irregularity of spike trains of the output neurons. Furthermore, the presence of the stochastic influence together with spike-timing-dependent plasticity could increase the correlation of the neurons. These effects would potentially contribute to the management of PD symptoms.

**Keywords:** Activity-dependent development of nervous systems, Spike-timing-dependent plasticity, coupled models in medical applications, Neuromorphic systems, Neurodegenerative diseases, Enhanced Hodgkin-Huxley models, Parkinson’s disease

## 1 Introduction

One of the most common neurodegenerative disorders of aging is Parkinson’s disease (PD), which is a progressive neurological degenerative disorder characterized by a severe loss of dopaminergic neurons in the substantia nigra pars compacta. PD is characterized by cardinal motor symptoms including slowness of movement (bradykinesia), akinesia, rigidity, and tremors at rest. Neuronal oscillations and symptoms of Parkinson’s disease (PD) are closely connected [20,7,34]. Many different treatments focus on the subthalamic nucleus (STN) to improve such motor symptoms, for instance, ablation surgery of STN or its fiber connections. Deep brain stimulation (DBS) of the STN has recently become an effective therapy for PD [20]. The DBS is a very impressive method [35] due to the fact that PD, characterized by the inadequacy of a chemical substance in the brain, can also be successfully treated with the passage of only electrical currents without a concomitant supply of biological or chemical reactions/factors. In general, biological neurons in the brains transmit information by generating spikes and such neurons are connected by synapses that process and store information. To better understand brain activities, we need to know how synapses work. In general, chemical synapses are more common in the brain, and these synapses do not physically join neurons [44,39]. To get closer to the real scenarios of brain activities, one needs to account for models of a synapse in which its synaptic strength changes as a function of the relative timing (i.e., time difference) between the spikes of the presynaptic and postsynaptic neurons, respectively. This change in the synaptic weight is known as spike-timing-dependent plasticity (STDP).

Many models have been proposed to analyze the dynamics of synaptic coupling of human brains in neurodegenerative disorders and therapeutic targets for such diseases. A model of STDP mediated by dopamine and its role in PD pathophysiology has been reported in [30]. For the first time, the results provided in [20]

have demonstrated that neuronal oscillations are predictive of DBS outcome. The DBS therapy for the noisy cortex and irresponsive subthalamus to improve parkinsonian locomotor activities has been reported in [26]. The authors in [43] have investigated the coupled effects of channels and synaptic dynamics in stochastic modelling of healthy and Parkinson’s-disease-affected brains. In [48], the authors have found that eSTDP and iSTDP restrict the balance of the excitatory–inhibitory balanced neuronal network and play a fundamental role in maintaining network stability and synchronization. Furthermore, their results would potentially also contribute to the guidance of the treatments and further research of neurodegenerative diseases. Moreover, the results reported in [36] show that STDP can support the multiplexing of rhythmic information. Additionally, STDP could demonstrate how to retain functionality despite continuous remodeling of all the synaptic weights.

The computational aspects of sensory information processing span from individual cells to the network level. The physical properties of single and small networks of nerve cells enable them to process and store information. Understanding of the cellular and dendritic mechanisms that could contribute to the processing of sensory information in single neurons has also been greatly increased. However, still very little is known about how the biophysical properties of single neurons are actually used to implement specific computations. Two types of neuronal computations thought to be fundamental to processing information within the nervous system are the multiplication of independent signals and invariance of neuronal responses. The evidence of a behaviorally induced form of synaptic plasticity that would encourage the development of fine-scale structured input patterns and the binding of features within single neurons has been presented in [31]. Feedforward inhibition is not only traditionally thought to sharpen the responses and temporal tuning of feedforward excitation onto principal neurons but also could also convey information used by single neurons to implement dendritic computations on sensory stimulus variables [47]. A discussion on the discrimination of the broad spatial statistics of synaptic inputs within the dendrites of a single neuron has been reported in [11]. Using the description based on single and dual dendritic recordings in vivo together with computational modelling, the membrane impedance of a collision detection neuron in the grasshopper *Schistocerca americana* has been characterized in [10]. A model of active dendritic integration and mixed neocortical network representations during an adaptive sensing behavior for single neurons has been considered in [32].

In the real scenarios in the neuronal models, the random fluctuations could affect the spiking activities of the neurons. In particular, stochastic factors arise through sensory fluctuations, brainstem discharges and thermal energy or random fluctuations at a microscopic level, such as the Brownian motion of ions. Such random fluctuations could cause burst discharges in brain systems. The brain rhythm bursts are enhanced by multiplicative noise [2]. The authors in [40] have investigated the effects of noise in gamma oscillations in a model of neuronal networks with different reversal potentials. Specifically, the presence of noise in a neuronal system can also be a solution in information processing [1,44]. The authors in [17] have shown that the detectability of weak signals in nonlinear systems (known as stochastic resonance) can be enhanced by random noise. Furthermore, they have also pointed out that the phase-based simplification of the STN neurons can accurately predict responses to temporally complex trains of inputs even when the perturbations in timing are large enough to obscure the oscillatory nature of the neuron’s firing. The question “Is this variation an unavoidable effect of generating spikes by sensory or synaptic processes (‘neural noise’) or is it an important part of the ‘signal’ that is transmitted to other neurons?” has been discussed in [38]. In general, the occurrence of synchronous events can emerge from the variety of mechanisms in physical systems. In neuronal networks, signal-evoked and intrinsic noise spike correlations both originate in the intricate connectivity of a neuronal network. Each cortical neuron receives inputs from approximately  $10^4$  other neurons and sends out signals via its synapses to about  $10^4$  others. In such a neuronal network, spiking cross-correlations in the activity of two neurons can emerge from direct synaptic connections or shared presynaptic partners. Because neurons are highly interconnected, it is almost unavoidable that two neurons in a network share some of their inputs. Just as multiple synaptic interaction structures can potentially give rise to the same pairwise correlations, a particular functional form of the spike correlation function may not be a unique signature of interneuronal interactions. In [21], the authors have shown that pairs of neurons receiving correlated input also exhibit correlations arising from precise spike-time synchronization by using simulations and experiments in rat hippocampal neurons. The role of input correlations in shaping the variability and noise correlations of evoked activity in the neocortex has been investigated in [3]. The effect of interpopulation STDP on synchronized rhythms in neuronal networks with inhibitory and excitatory populations has been discussed

in [24]. The authors in [48] have consider the synchronization and oscillation behaviors of excitatory and inhibitory populations with STDP.

This paper is built upon and extend the recent works [44,39,43], where the authors considered the static synapses whose weights are fixed and the dynamic synapses whose synaptic strength is dependent on the recent spike history (short-term plasticity). However, in real brain models, the strength of connections between neurons in the brain is based on the relative timing of a particular neuron’s output and input action potentials. Drawing from the fields of PD studies and the effects of natural random factors in biological system dynamics, we develop and investigate a model of coupled effects of channels and synaptic dynamics by using stochastic modelling of healthy brain cells with applications in PD. In particular, we consider a cell membrane potential model in the STN part of the human brain. Our analysis focuses on considering a Langevin stochastic equation in a numerical setting for a cell membrane potential with random inputs and input correlations under the influence of STDP. We discuss the role of STDP in neuromorphic systems. Next, we provide numerical examples and discuss the effects of random inputs on the time evolution of the STN cell membrane potential as well as the spiking activities of the STN neuron. Our numerical results indicate that STDP enhances the regularity of interspike intervals (ISI) in the spike trains of output neurons. However, the presence of a random refractory period, along with random input currents, may significantly increase the irregularity of these spike trains. Additionally, the combination of stochastic influences and STDP could enhance the correlation among neurons. These effects may contribute to the management of Parkinson’s disease symptoms.

## 2 Model description

STDP is a fundamental mechanism in the brain that modifies the synaptic strengths between neurons based on the coincidence of pre- and postsynaptic spikes. In conventional asymmetric forms of STDP, the temporal order of spikes is critical, so that when the presynaptic spike precedes the postsynaptic spike (i.e., pre-post pairing), the STDP rule leads to long-term potentiation (LTP) of the synapse between pre- and postsynaptic neurons, whereas long-term depression (LTD) is induced in the reverse scenario (i.e., post-pre pairing). Although STDP is a local mechanism and merely depends on the pre- and postsynaptic spike timings, it can determine global connectivity patterns emerging in recurrent neuronal networks.

We will focus on building a model of a synapse in which its synaptic strength changes as a function of the relative timing (i.e., time difference) between the spikes of the presynaptic and postsynaptic neurons, respectively. This change in the synaptic weight is known as STDP. The aims of this paper are to build a model of synapse that show STDP and study how correlations in input spike trains influence the distribution of synaptic weights. We will model the presynaptic input as Poisson-type spike trains. The postsynaptic neuron will be modeled as an HH neuron.

We assume that a single postsynaptic neuron is driven by  $N$  presynaptic neurons. That is, there are  $N$  synapses, and we will study how their weights depend on the statistics or the input spike trains and their timing with respect to the spikes of the postsynaptic neuron.

The phenomenology of STDP is generally described as a biphasic exponentially decaying function. That is, the instantaneous change in weights is given by:

$$\Delta W = A_+ e^{(t_{\text{pre}} - t_{\text{post}})/\tau_+} \text{ if } t_{\text{post}} > t_{\text{pre}}, \quad (1)$$

$$\Delta W = -A_- e^{-(t_{\text{pre}} - t_{\text{post}})/\tau_-} \text{ if } t_{\text{post}} < t_{\text{pre}}, \quad (2)$$

where  $\Delta W$  denotes the change in the synaptic weight,  $A_+$ ,  $A_-$  determine the maximum amount of synaptic modification (which occurs when the timing difference between presynaptic and postsynaptic spikes is close to zero), while  $\tau_+$  and  $\tau_-$  represent the ranges of pre-to-postsynaptic interspike intervals over which synaptic strengthening or weakening occurs. Thus,  $\Delta W > 0$  means that the postsynaptic neuron spikes after the presynaptic neuron.

This model captures the phenomena that repeated occurrences of presynaptic spikes within a few milliseconds before postsynaptic action potentials lead to long-term potentiation (LTP) of the synapse, whereas repeated occurrences of presynaptic spikes after the postsynaptic ones lead to long-term depression (LTD) of the same synapse.

The latency between presynaptic and postsynaptic spike ( $\Delta t$ ) is defined as:

$$\Delta t = t_{\text{pre}} - t_{\text{post}}, \quad (3)$$

where  $t_{\text{pre}}$  and  $t_{\text{post}}$  are the timings of the presynaptic and postsynaptic spikes, respectively.

## 2.1 Keeping track of pre- and postsynaptic spikes

Since a neuron will receive numerous presynaptic spike inputs, in order to implement STDP by taking into account different synapses, we first have to keep track of the pre- and postsynaptic spike times throughout the simulation.

A convenient way to do this is to define the following equation for each postsynaptic neuron:

$$\tau_- \frac{dM}{dt} = -M \quad (4)$$

and whenever the postsynaptic neuron spikes, we have

$$M(t) = M(t) - A_-. \quad (5)$$

This way  $M(t)$  tracks the number of postsynaptic spikes over the timescale  $\tau_-$ .

Similarly, for each presynaptic neuron, we define:

$$\tau_+ \frac{dP}{dt} = -P \quad (6)$$

and whenever there is a spike on the presynaptic neuron, we have

$$P(t) = P(t) + A_+. \quad (7)$$

The variables  $M(t)$  and  $P(t)$  are very similar to the equations for the synaptic conductances, i.e.,  $g_i(t)$ , except that they are used to keep track of pre- and postsynaptic spike times on a much longer timescale. Note that,  $M(t)$  is always negative, and  $P(t)$  is always positive. You can probably already guess that  $M$  is used to induce LTD and  $P$  to induce LTP because they are updated by  $A_-$  and  $A_+$ , respectively.

Important note:  $P(t)$  depends on the presynaptic spike times. If we know the presynaptic spike times,  $P$  can be generated before simulating the postsynaptic neuron and the corresponding STDP weights.

## 2.2 Implementation of STDP

We will change the value of the peak synaptic conductance based on the presynaptic and postsynaptic timing, thus using the variables  $M(t)$  and  $P(t)$ .

Each synapse  $i$  has its own peak synaptic conductance ( $\bar{g}_i$ ), which may vary between  $[0, \bar{g}_{\text{max}}]$ , and will be modified depending on the presynaptic and postsynaptic timing.

1. When the  $i$ th presynaptic neuron elicits a spike, its corresponding peak conductance is updated according to the following equation:

$$\bar{g}_i = \bar{g}_i + M(t)\bar{g}_{\text{max}}. \quad (8)$$

Note that,  $M(t)$  tracks the time since the last postsynaptic potential and is always negative. Hence, if the postsynaptic neuron spikes shortly before the presynaptic neuron, the above equation shows that the peak conductance will decrease.

2. When the postsynaptic neuron spikes, the peak conductance of each synapse is updated according to:

$$\bar{g}_i = \bar{g}_i + P(t)\bar{g}_{\text{max}}. \quad (9)$$

Note that,  $P(t)$  tracks the time since the last spike of  $i$ th pre-synaptic neuron and is always positive. Thus, the equation given above shows that if the presynaptic neuron spikes before the postsynaptic neuron, its peak conductance will increase.

### 2.3 The leaky integrate-and-fire neuron connected with synapses that show STDP

We connect  $N$  presynaptic neurons to a single postsynaptic neuron. We do not need to simulate the dynamics of each presynaptic neuron as we are only concerned about their spike times. So, we will generate  $N$  Poisson-type spikes. Here, we will assume that all these inputs are excitatory.

We need to simulate the dynamics of the postsynaptic neuron as we do not know its spike times. We model the postsynaptic neuron as Hodgkin-Huxley (HH) system modelling an STN cell membrane potential.

Furthermore, motivated by [37,50,49,25], we consider a modified HH system modelling a STN cell membrane potential. In particular, we first choose a STN healthy cell, then switch to a PD cell, and study the effects of random inputs on the STN cell membrane potential under synaptic conductance dynamics.

In biological systems of brain networks, instead of physically joined neurons, a spike in the presynaptic cell causes a release of a chemical, or a neurotransmitter. Neurotransmitters are released from synaptic vesicles into a small space between the neurons called the synaptic cleft [15]. In what follows, we will investigate the chemical synaptic transmission and study how excitation and inhibition affect the patterns in the neurons' spiking output in our HH model.

In this section, we consider a HH model of synaptic conductance dynamics. In particular, neurons receive a myriad of excitatory and inhibitory synaptic inputs at dendrites. To better understand the mechanisms of synaptic conductance dynamics, we use the description of Poissonian trains to investigate the dynamics of the random excitatory (E) and inhibitory (I) inputs to a neuron [8,27].

We consider the transmitter-activated ion channels as an explicitly time-dependent conductivity ( $g_{\text{syn}}(t)$ ). The conductance transients can be defined by the following equation (see, e.g., [8,15]):

$$\frac{dg_{\text{syn}}(t)}{dt} = -\bar{g}_i \sum_k \delta(t - t_k) - \frac{g_{\text{syn}}(t)}{\tau_{\text{syn}}}, \quad (10)$$

where  $\bar{g}_{\text{syn}}$  (synaptic weight) denotes the maximum conductance elicited by each incoming spike, while  $\tau_{\text{syn}}$  is the synaptic time constant, and  $\delta(\cdot)$  is the Dirac delta function. Note that the summation runs over all spikes received by the neuron at time  $t_k$ . We have the following formula for converting conductance changes to the current by using Ohm's law:

$$I_{\text{syn}}(t) = g_{\text{syn}}(t)(V(t) - E_{\text{syn}}), \quad (11)$$

where  $V$  is the membrane potential, while  $E_{\text{syn}}$  represents the direction of current flow and the excitatory or inhibitory nature of the synapse.

The total synaptic input current  $I_{\text{syn}}$  is the combination of both excitatory and inhibitory inputs. Assume that the total excitatory and inhibitory conductances received at time  $t$  are  $g_E(t)$  and  $g_I(t)$ , and their corresponding reversal potentials are  $E_E$  and  $E_I$ , respectively. Then, the total synaptic current can be defined by the following equation (see, e.g., [27]):

$$I_{\text{syn}}(V(t), t) = -g_E(t)(V - E_E) - g_I(t)(V - E_I) = -I_E - I_I. \quad (12)$$

In [37], the authors have used the quantity  $I_{\text{GPe,STN}}$  in the STN model. However, we know that STN-DBS generate both excitatory and inhibitory postsynaptic potentials in STN neurons [4]. In our current consideration, instead of using the current  $I_{\text{GPe,STN}}$ , we consider the current  $I_{\text{STN,DBS}} = -I_E - I_I$ . Let us define the following synaptic dynamics of the STN cell membrane potential ( $V$ ) described by the following model (based on [37])

$$C_m \frac{d}{dt} V(t) = -I_L - I_{\text{Na}} - I_K - I_T - I_{\text{Ca}} - I_{\text{ahp}} - I_{\text{STN,DBS}} + I_{\text{app}} + I_{\text{dbs}} \quad \text{if } V(t) \leq V_{\text{th}}, \quad (13)$$

$$V(t) = V_{\text{reset}} \quad \text{otherwise}, \quad (14)$$

where  $I_{\text{app}}$  is the external input current, while  $C_m$  is the membrane capacitance and  $t \in [0, T]$ . Additionally, in (13),  $V_{\text{th}}$  denotes the membrane potential threshold to fire an action potential.

In this model, we assume that a spike takes place whenever  $V(t)$  crosses  $V_{\text{th}}$  in the STN membrane potential. In that case, a spike is recorded and  $V(t)$  resets to  $V_{\text{reset}}$  value. Hence, the reset condition is summarized by  $V(t) = V_{\text{reset}}$  if  $V(t) \geq V_{\text{th}}$ . The quantity  $I_{\text{ahp}}$  represents the calcium-activated potassium current for the spike after hyperpolarization in STN.

The concentration of intracellular  $\text{Ca}^{2+}$  is governed by the following calcium balance equation

$$\frac{d}{dt}Ca(t) = \varepsilon(I_{\text{Ca}} - I_T - k_{\text{Ca}}Ca(t)), \quad (15)$$

where  $\varepsilon = 3.75 \times 10^{-5}$  is a scaling constant,  $k_{\text{Ca}} = 22.5 \text{ (ms}^{-1}\text{)}$  is a given time constant (see, e.g., [45,6]).

Furthermore, we consider an external random (additive noise) input current as follows:  $I_{\text{app}} = \mu_{\text{app}} + \sigma_{\text{app}}\eta(t)$ , where  $\eta$  is the zero-Gaussian white noise with  $\mu_{\text{app}} > 0$  and  $\sigma_{\text{app}} > 0$ . Using the description of such random input current in our system, the first equation (13) can be considered as the following Langevin stochastic equation (see, e.g., [33]):

$$\begin{aligned} C_m \frac{d}{dt}V(t) &= -I_L - I_{\text{Na}} - I_{\text{K}} - I_T - I_{\text{Ca}} - I_{\text{ahp}} - I_{\text{E}} - I_{\text{I}} \\ &\quad + I_{\text{dbs}} + \mu_{\text{app}} + \sigma_{\text{app}}\eta(t) \quad \text{if } V(t) \leq V_{\text{th}}. \end{aligned} \quad (16)$$

Therefore, the system (13)–(15) ( $t \in [0, T]$ ) can be rewritten as

$$\begin{aligned} C_m \frac{d}{dt}V(t) &= -I_L - I_{\text{Na}} - I_{\text{K}} - I_T - I_{\text{Ca}} - I_{\text{ahp}} - I_{\text{E}} - I_{\text{I}} \\ &\quad + I_{\text{dbs}} + \mu_{\text{app}} + \sigma_{\text{app}}\eta(t) \quad \text{if } V(t) \leq V_{\text{th}}, \end{aligned} \quad (17)$$

$$V(t) = V_{\text{reset}} \quad \text{otherwise.} \quad (18)$$

Furthermore, we consider the following gating variable dynamics (see, e.g., [37])

$$\frac{d}{dt}h(t) = 0.75 \frac{h_{\infty}(V) - h(t)}{\tau_h(V)}, \quad (19)$$

$$\frac{d}{dt}n(t) = 0.75 \frac{n_{\infty}(V) - n(t)}{\tau_n(V)}, \quad (20)$$

$$\frac{d}{dt}r(t) = 0.2 \frac{r_{\infty}(V) - r(t)}{\tau_r(V)}, \quad (21)$$

$$\frac{d}{dt}c(t) = 0.08 \frac{c_{\infty}(V) - c(t)}{\tau_c(V)}, \quad (22)$$

$$\frac{d}{dt}Ca(t) = \varepsilon(I_{\text{Ca}} - I_T - k_{\text{Ca}}Ca(t)). \quad (23)$$

The initial data we use for the system (17)–(23) define its initial conditions:

$$V(0) = V_0, \quad (24)$$

$$h(0) = h_\infty(V_0), \quad (25)$$

$$n(0) = n_\infty(V_0), \quad (26)$$

$$r(0) = r_\infty(V_0), \quad (27)$$

$$c(0) = c_\infty(V_0), \quad (28)$$

$$Ca(0) = \frac{a_\infty(V_0)}{a_\infty(V_0) + b_\infty(V_0)}, \quad (29)$$

where  $h_\infty, n_\infty, r_\infty, c_\infty, a_\infty, b_\infty$  are described as in Table 1.

In our model (17)–(29), as we mentioned above, we use the simplest input spike train with Poisson process in which the stochastic process of interest provides a suitable approximation to stochastic neuronal firings [42]. The input spikes will be carried out by the quantity  $\sum_k \delta(t - t_k)$  in the equation (10) and the input spikes are given when every input spike arrives independently of other spikes. The process will be described as follows:

- For designing a spike generator of spike train, we define the probability of firing a spike within a short interval (see, e.g. [8]) as  $P(1 \text{ spike during } \Delta t) = r_j \Delta t$ , where  $j = e, i$  with  $r_e, r_i$  representing the instantaneous excitatory and inhibitory firing rates, respectively.
- Then, a Poisson spike train is generated by first subdividing the time interval into a group of short sub-intervals through small time steps  $\Delta t$ . In our model, we use  $\Delta t = 0.1$  (ms).
- We define a random variable  $x_{\text{rand}}$  with uniform distribution over the range between 0 and 1 at each time step.
- Finally, we compare the random variable  $x_{\text{rand}}$  with the probability of firing a spike, which reads:

$$\begin{cases} r_j \Delta t > x_{\text{rand}}, & \text{generates a spike,} \\ r_j \Delta t \leq x_{\text{rand}}, & \text{no spike is generated.} \end{cases} \quad (30)$$

By using model (17)–(29), we also investigate the effects of random refractory periods. We consider the random refractory periods  $t_{\text{ref}}$  as  $t_{\text{ref}} = \mu_{\text{ref}} + \sigma_{\text{ref}} \tilde{\eta}(t)$ , where  $\tilde{\eta}(t) \sim \mathcal{N}(0, 1)$  is the standard normal distribution,  $\mu_{\text{ref}} > 0$  and  $\sigma_{\text{ref}} > 0$ .

In general, the information on stimulating activities in a neuron can be provided by the irregularity of spike trains. The time interval between adjacent spikes is called the ISI. The coefficient of variation (CV) of the ISI in a cell membrane potential with multiple inputs can bring useful information about the output of a decoded neuron. In what follows, we will demonstrate that when we increase the value of  $\sigma_{\text{ref}}$ , the irregularity of the spike trains increases (see also [12]). The spike irregularity of spike trains can be described via the coefficient of variation of the inter-spike-interval (see, e.g., [5,12]) as follows:

$$CV_{\text{ISI}} = \frac{\sigma_{\text{ISI}}}{\mu_{\text{ISI}}}, \quad (31)$$

where  $\sigma_{\text{ISI}}$  is the standard deviation and  $\mu_{\text{ISI}}$  is the mean of the ISI of an individual neuron.

In the next section, let us consider the output firing rate as a function of Gaussian white noise mean or direct current value, namely, the input-output transfer function of the neuron.

In our model, we choose the parameter set as in the following Table 1:

Since these parameters have also been used in [37] for STN cell membrane potential experiments, we take them for our model validation. Moreover, in our consideration, we use not only the parameters from Table 1, but also the following parameters:  $V_{\text{th}} = -55$  (mV),  $V_{\text{reset}} = -70$  (mV),  $V_0 = -65$  (mV),  $\Delta t = 0.1$ ,  $C_m = 10$  (nF),  $\tau_E = 2$  (ms),  $\tau_I = 5$  (ms),  $\bar{g}_E = 1.5$  (nS),  $\bar{g}_I = 0.5$  (nS),  $r_e = 10$ ,  $r_i = 10$ ,  $n_E = 20$  spike trains,  $n_I = 80$  spike trains. Here,  $n_E$  and  $n_I$  represent the number of excitatory and inhibitory presynaptic spike trains, respectively.

Mathematically, the developed model (17)–(29) is an evolutionary system that combines stochastic differential equations and ordinary differential equations (SDEs-ODEs), where the stochastic membrane potential equation is coupled to the activation and inactivation ion channels equations, as well as to the calcium-activated potassium current equation. This system can be considered as a modified HH system.

**Table 1.** Steady-state functions for channel gating variables and time constants for the different ion channels (see, e.g., [37]).

Current	Gating variables	Gating variables	Parameters
$I_L = g_L(v - E_L)$			$g_L = 2.25$ (nS) $E_L = -60$ (mV)
$I_{Na} = g_{Na}m_\infty^3(V)h(V)(V - E_{Na})$	$m_\infty(V) = 1/(1 + \exp(-\frac{V+30}{15}))$	$h_\infty(V) = 1/(1 + \exp(-\frac{V+39}{3.1}))$ $\tau_h(V) = 1 + 500/(1 + \exp(-\frac{V+57}{-3}))$	$g_{Na} = 37$ $E_{Na} = 55$ (mV)
$I_K = g_Kn^4(V)(V - E_K)$	$n_\infty(V) = 1/(1 + \exp(-\frac{V+32}{8}))$ $\tau_n(V) = 1 + 100/(1 + \exp(-\frac{V+80}{-26}))$		$g_K = 45$ (nS) $E_K = -80$ (mV)
$I_T = g_Ta_\infty^3(V)b_\infty^2(r)r(V)(V - E_T)$	$a_\infty(V) = 1/(1 + \exp(-\frac{V+63}{7.8}))$ $b_\infty(V) = 1/(1 + \exp(-\frac{V-0.4}{0.1}))$ $-1/(1 + \exp(4))$	$r_\infty(V) = 1/(1 + \exp(\frac{V+67}{2}))$ $\tau_r(V) = 7.1 + 17.5/(1 + \exp(-\frac{V+68}{-2.2}))$	$g_T = 0.5$ (nS) $E_T = 0$ (mV)
$I_{Ca} = g_{Ca}c^2(V)(V - E_{Ca})$	$c_\infty(V) = 1/(1 + \exp(-\frac{V+20}{8}))$ $\tau_c(V) = 1 + 10/(1 + \exp(\frac{V+80}{26}))$		$g_{Ca} = 2$ (nS) $E_{Ca} = 140$ (mV)
$I_{ahp} = g_{ahp}(V - E_{ahp})(\frac{Ca}{Ca+15})$			$g_{ahp} = 20$ (nS) $E_{ahp} = -80$ (mV)
$I_{dbs} = 5 + 5 \sin(2\pi t)$ (pA)			

## 2.4 Effects of input correlations

Correlation or synchrony in neuronal activity can be described for any readout of brain activity. Here, we are concerned with the spiking activity of neurons.

In the simplest way, correlation/synchrony refers to the coincident spiking of neurons, i.e., when two neurons spike together, they are firing in synchrony or are correlated. Neurons can be synchronous in their instantaneous activity, i.e., they spike together with some probability. However, it is also possible that a neuron's spiking at time  $t$  is correlated with the spikes of another neuron with a delay (time-delayed synchrony).

Origin of synchronous neuronal activity:

- Common inputs, i.e., two neurons are receiving input from the same sources. The degree of correlation of the shared inputs is proportional to their output correlation.
- Pooling from the same sources. Neurons do not share the same input neurons but are receiving inputs from neurons which themselves are correlated.
- Neurons are connected to each other (uni- or bi-directionally): This will only give rise to time-delayed synchrony. Neurons could also be connected via gap-junctions.
- Neurons have similar parameters and initial conditions.

When neurons spike together, they can have a stronger impact on downstream neurons. Synapses in the brain are sensitive to the temporal correlations (i.e., delay) between pre- and postsynaptic activity, and this, in turn, can lead to the formation of functional neuronal networks - the basis of unsupervised learning.

Synchrony implies a reduction in the dimensionality of the system. In addition, correlations, in many cases, can impair the decoding of neuronal activity.

A simple model to study the emergence of correlations is to inject common inputs into a pair of neurons and measure the output correlation as a function of the fraction of common inputs.

Here, we are going to investigate the transfer of correlations by computing the correlation coefficient of spike trains recorded from two unconnected HH neurons, which received correlated inputs.

The input current to HH neuron  $i = 1, 2$  is

$$I_i = \mu_i + \sigma_i(\sqrt{1 - c}\xi_i + \sqrt{c}\xi_c), \quad (32)$$

where  $\mu_i$  is the temporal average of the current. The Gaussian white noise  $\xi_i$  is independent for each neuron, while  $\xi_c$  is common to all neurons. The variable  $c$  ( $0 \leq c \leq 1$ ) controls the fraction of common and independent inputs.  $\sigma_i$  shows the variance of the total input.

The sample correlation coefficient between two input currents,  $I_i$  and  $I_j$ , is defined as the sample covariance of  $I_i$  and  $I_j$  divided by the square root of the sample variance of  $I_i$  multiplied by the square root of the sample



variance of  $I_j$ . We consider the following equations:

$$r_{ij} = \frac{\text{cov}(I_i, I_j)}{\sqrt{\text{var}(I_i)}\sqrt{\text{var}(I_j)}}, \quad (33)$$

$$\text{cov}(I_i, I_j) = \sum_{k=1}^L (I_i^k - \bar{I}_i)(I_j^k - \bar{I}_j), \quad (34)$$

$$\text{var}(I_i) = \sum_{k=1}^L (I_i^k - \bar{I}_i)^2, \quad (35)$$

where  $\bar{I}_i$  is the sample mean,  $k$  is the time bin, and  $L$  is the length of  $I$ . This means that  $I_i^k$  is current at  $i$  at time  $k \cdot dt$ . Note that the equations above are not accurate for sample covariances and variances as they should be additionally divided by  $L - 1$ . We have dropped this term because it cancels out in the sample correlation coefficient formula.

## 2.5 STDP in neuromorphic systems and other applications

With many current and potential applications, STDP is often thought of as an unsupervised brain-like learning mechanism for spiking neural networks (SNNs) that, among other things, has attracted significant attention from the neuromorphic hardware community [41,29]. Its ability to mimic biological learning processes makes STDP highly relevant for various applications, including pattern recognition and sensory processing, real-time pattern recognition, stabilized supervised STDP, and synchronization in neural networks. Many models have been proposed to investigate the role of STDP mechanisms across these applications. For example, the human brain is recognized as the most complex entity in the known universe [19]. At the microcircuit level, neuronal cells are organized into layers with various connectivity motifs. While the information processing mechanisms at this level remain not fully understood, investigating these motifs—particularly about STDP—is essential for gaining insights into biological learning mechanisms and the emergence of intelligence. STDP is an unsupervised brain-like learning rule implemented in many SNNs and neuromorphic chips. However, a significant performance gap exists between ideal model simulation and neuromorphic implementation. STDP is implemented in SNNs and neuromorphic chips, serving as an unsupervised learning rule crucial for mimicking brain-like information processing [18]. Its applications include noisy spatiotemporal spike pattern detection, which is particularly effective even with low-resolution synaptic efficacy in neuromorphic implementations. This capability enhances performance in various computational tasks, making STDP relevant for advancing neuromorphic hardware [13,14]. STDP is used to train an efficient Spiking Auto-Encoder that leverages asynchronous sparse spikes for input reconstruction, denoising, and classification, achieving superior performance with significantly fewer spikes compared to state-of-the-art methods. On the other hand, STDP has significant applications in bio-plausible meta-learning models, particularly in enhancing the adaptability and efficiency of machine-learning systems. By incorporating STDP and Reward-Modulated STDP, these models reflect biological learning mechanisms and enable quick learning in low-data scenarios. This approach is particularly useful for preventing catastrophic forgetting in meta-learning tasks, allowing the model to retain previously acquired knowledge while learning new tasks. Additionally, STDP facilitates the application of these models in spike-based neuromorphic devices, improving their performance in tasks such as few-shot classification and advancing AI systems' capabilities to mimic human-like learning [23]. STDP is employed to train a Spiking Auto-Encoder that efficiently performs input reconstruction, denoising, and classification with minimal spike usage, showcasing enhanced performance on image datasets while maintaining competitiveness against other learning approaches [46]. STDP is also applied through memristors as synapses to enable in situ learning and inference in SNNs. This approach addresses the computational challenges associated with implementing STDP in hardware, allowing for efficient weight modulation that enhances speed and reduces power consumption. The integration of STDP facilitates real-time pattern recognition by employing a winner-takes-all mechanism within the SNN architecture. The proposed design significantly improves performance metrics, including power, energy, and accuracy, enabling the classification of 50 million images per second [22]. STDP is employed in the Stabilized Supervised STDP learning rule to enhance the classification layer of SNNs, integrating unsupervised STDP for feature extraction and improving performance on image recognition tasks [16]. Furthermore, STDP is utilized to investigate the configurations needed to achieve robust synchronization

in neural networks, with findings that could inform the design of neuromorphic circuits for improved information processing and transmission through synchronization phenomena [51]. Overall, despite the challenges in scaling STDP for deeper networks and larger tasks, its biological relevance and versatility highlight its significance in advancing artificial intelligence and neural computation. STDP holds the potential to enhance the performance of robotic systems by allowing them to learn from their environments in real time, reinforcing its critical role in the development of intelligent systems.

### 3 Numerical results

In this section, we take a single STN neuron and study how the neuron behaves under random inputs and when it is bombarded with both excitatory and inhibitory spike trains together with the influence of STDP. The numerical results reported in this section have been obtained using a discrete-time integration based on the Euler method implemented in Python.

In particular, we use the coupled SDEs-ODEs system (2.8)–(2.20) that describes the dynamics of the STN membrane potential. As we have mentioned in the previous section, we will focus on the effects of Gaussian white noise input current together with the random refractory periods on the STN cell membrane potential.

The main numerical results of our analysis are shown in Figs 2 - 8, where we have plotted the time evolution of the membrane potential calculated based on model (17)-(29), along with the spike count profile, the corresponding spike irregularity profile and the effects of input correlations on the output correlations for STN healthy and PD cells with STDP. We investigate the effects of additive type of random input currents in the presence of a random refractory period and the input correlations in a modified HH neuron under synaptic conductance dynamics with STDP. We observe that the spiking activity of a neuron in the STN cell membrane potential is influenced by random external currents, random refractory periods, STDP, and input correlations.

In order to switch from healthy conditions to Parkinsonian conditions in the basal ganglia model, we consider a decrease in the current  $I_{app}$  applied to the STN. In particular, we have  $I_{app} = 33$  (pA) for a healthy STN cell and  $I_{app} = 23$  (pA) for a Parkinsonian STN cell (see, e.g., [37]). Therefore, an STN cell in the case of injected current input  $I_{app} = 33$  (pA) results in a healthy STN cell, while an STN cell in the case of injected current  $I_{app} = 23$  (pA) is considered as a PD-affected STN cell.

In particular, we look at the Fig. 2, where we have plotted the time evolution of the STN cell membrane potential with direct input current and direct refractory period of healthy cells. The neuron spikes are different between the neuron spikes in the case of healthy cells and with PD cells presented in Figs. 2-3. There are missing spikes in the time interval of  $[0, 35]$  in Fig. 3.

In Fig. 4, in the case of healthy cell, we added the random input current and random refractory period to the system. We observe that there are fluctuations in the time evolution of the membrane potential, the total excitatory synaptic conductance as well as the trace of the number of postsynaptic spikes over the timescale  $\tau_-$ . In the case of PD-affected cells with random input current and random refractory period in Fig. 5, we see that the time evolution of the cell membrane potential is more unstable. There are also fluctuations in the trace of the number of postsynaptic conductance and the total excitatory synaptic conductance.

In Fig. 6, we consider a DBS input to the system, there are still fluctuations in the time evolution of the membrane potential and the trace of the number of postsynaptic spikes over the timescale  $\tau_-$ . In what follows, we also look at the corresponding ISI distributions and the spike irregularity profiles of the cases presented in Fig. 7.

In Fig. 7, we present spiking irregularity profiles in the case of an additive noise input current, along with the ISI distribution for healthy and Parkinson's disease (PD)-affected cells. The variability in ISI is typically measured by its coefficient of variation,  $CV_{ISI}$ . Our analysis focuses on values at  $I_{app} = 23$  pA and  $I_{app} = 33$  pA. We first determine the average current injection values,  $I_{average} = [22, 34]$  pA. The ISI is computed by identifying the spike times and calculating the differences between them. The  $CV_{ISI}$  is then defined as per equation (31).

In Fig. (7), we observe a trend where spike irregularity increases from left to right and decreases from top to bottom. PD cells exhibit greater spike irregularity compared to healthy cells, with a corresponding increase in the ISI range of  $CV_{ISI}$ . It is evident that the presence of a random refractory period significantly influences the spiking activity, reducing irregularity. Additionally, we observe that STDP in the modified HH

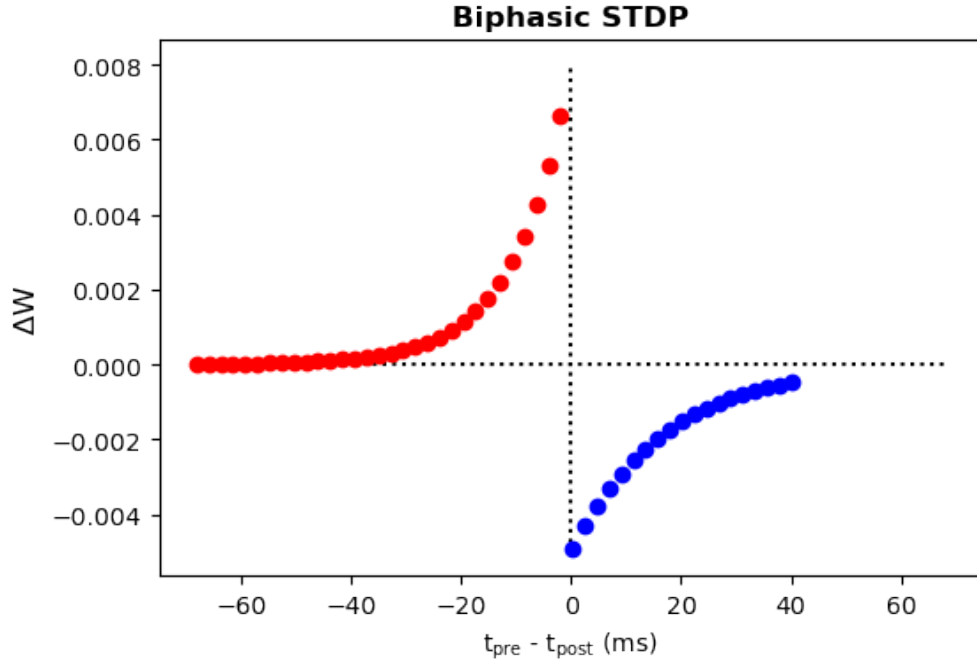


**Fig. 1.** [Color online] The change in the synaptic weight.

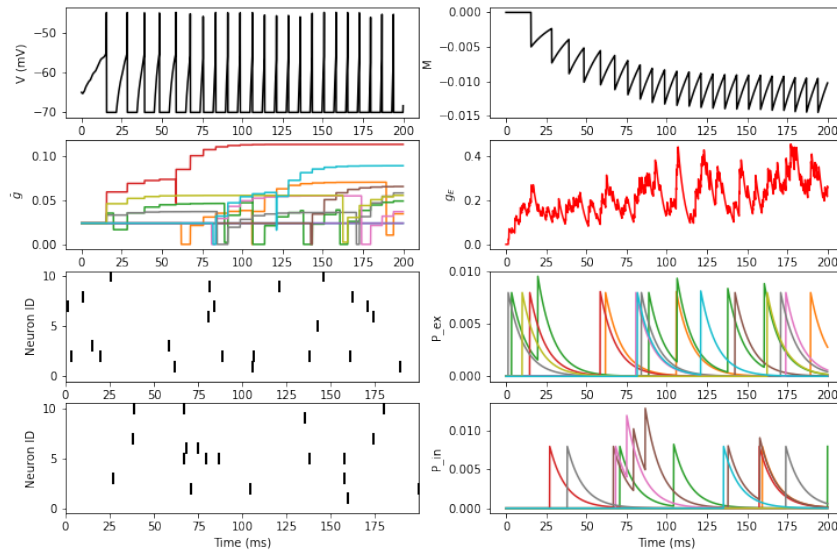


**Fig. 2.** [Color online] Membrane potential profile of direct input current and direct refractory period of healthy cells.

model increases the ISI of spike trains in output neurons, in contrast to the model without STDP, as reported in [43]. Moreover, combining a random refractory period with DBS further reduces spike irregularity.

Let us combine the two procedures above. First, we generate the correlated inputs. Then we inject the correlated inputs  $I_1$  and  $I_2$  into a pair of neurons and record their output spike times. We continue measuring

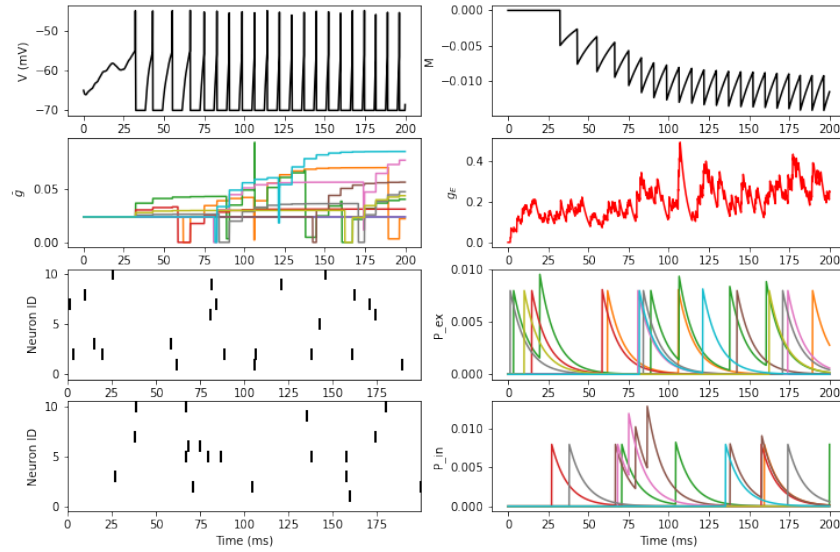


**Fig. 3.** [Color online] Membrane potential profile of direct input current and direct refractory period of PD.

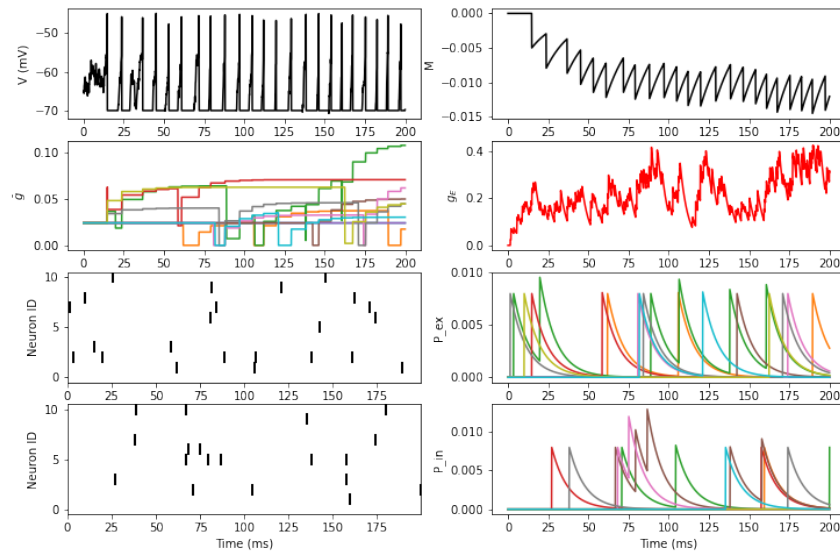


**Fig. 4.** [Color online] Membrane potential profile of direct input current and direct refractory period of healthy cells. Parameters:  $\sigma = 1, \sigma_{ref} = 1$ .

the correlation between the outputs and investigate the relationship between the input correlation and the output correlation.

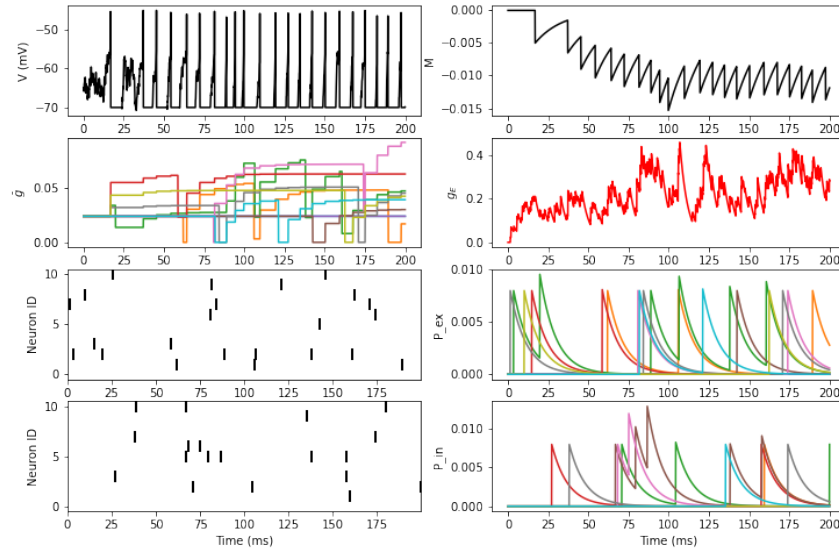


**Fig. 5.** [Color online] Membrane potential profile of random input current and random refractory period of PD. Parameters:  $\sigma = 1, \sigma_{\text{ref}} = 1$ .

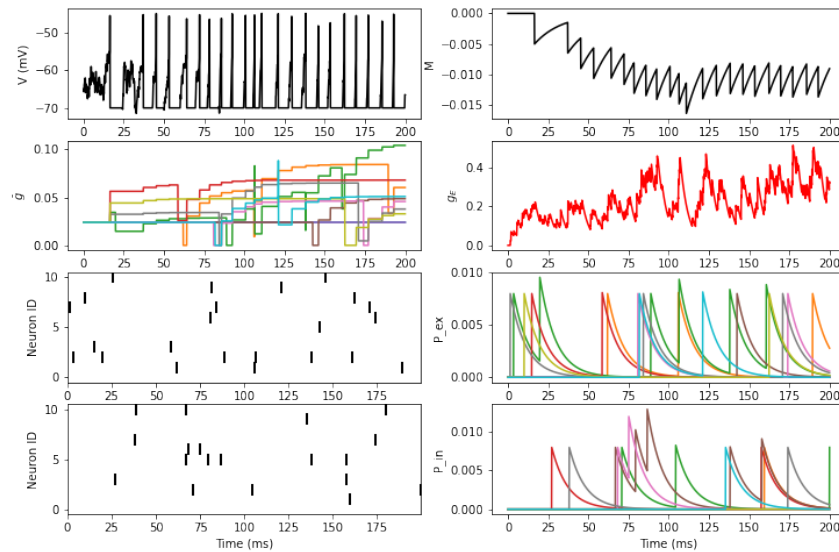


**Fig. 6.** [Color online] Membrane potential profile of random input current and random refractory period of PD cells with DBS.

In Fig. 8, the plot of input correlation versus output correlation is referred to as the correlation transfer function of neurons. The results indicate that output correlation is lower than input correlation and output correlation varies linearly with input correlation.

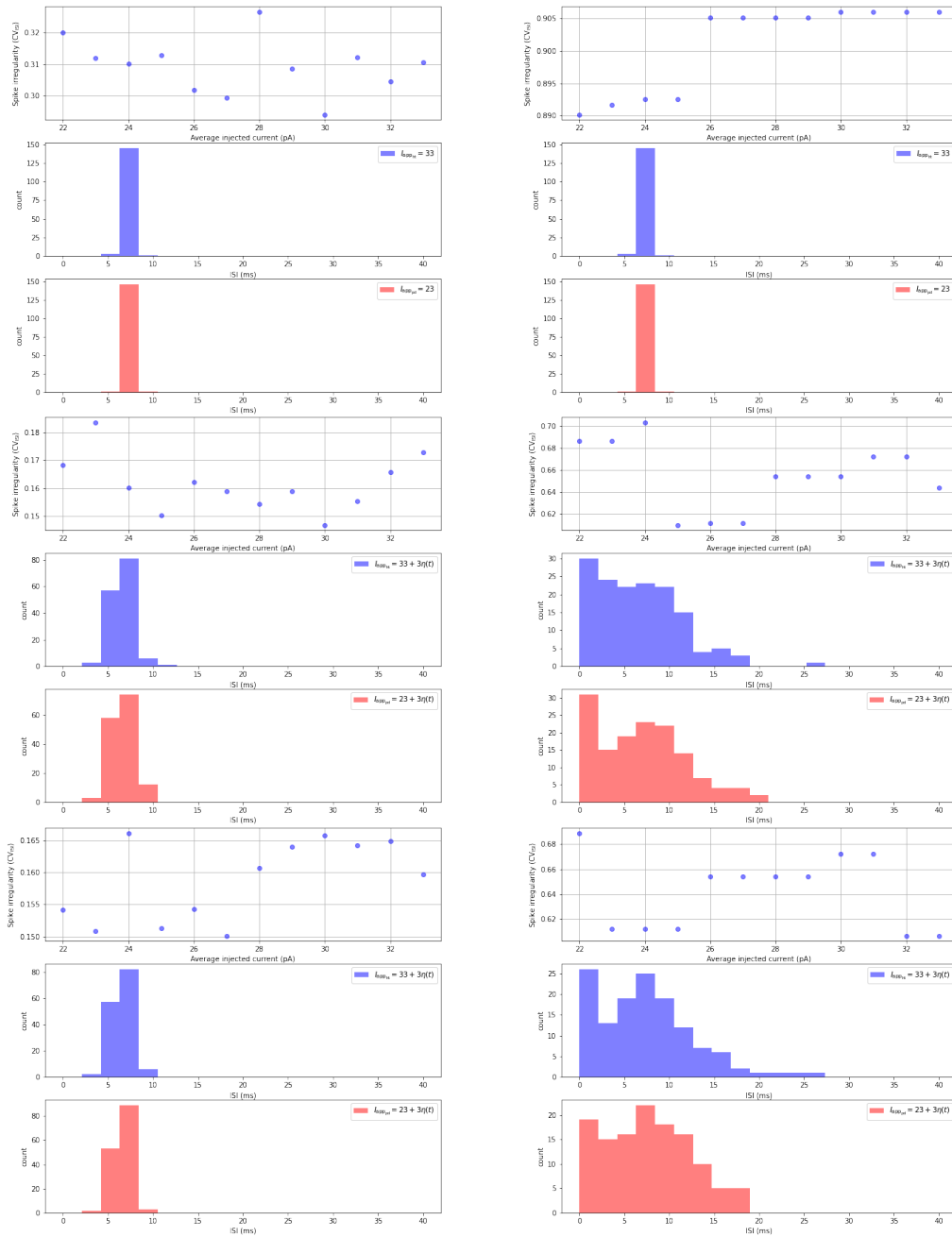


**Fig. 7.** Spike irregularity profiles in the case with the additive noise input current and the ISI distribution. From the top to the bottom, first 3 rows: ISI distributions with direct refractory period. Second 3 rows: ISI distributions with random refractory period. Last 3 rows: ISI distributions with random refractory period and DBS. Parameters: with  $\sigma = 1, \sigma_{\text{ref}} = 1$  in the left panel, and  $\sigma = 10, \sigma_{\text{ref}} = 5$  in the right panel.

When input correlations do not affect the neuron’s capacity, output correlation remains independent of both the mean and standard deviation. However, we observe that increasing the standard deviation of the

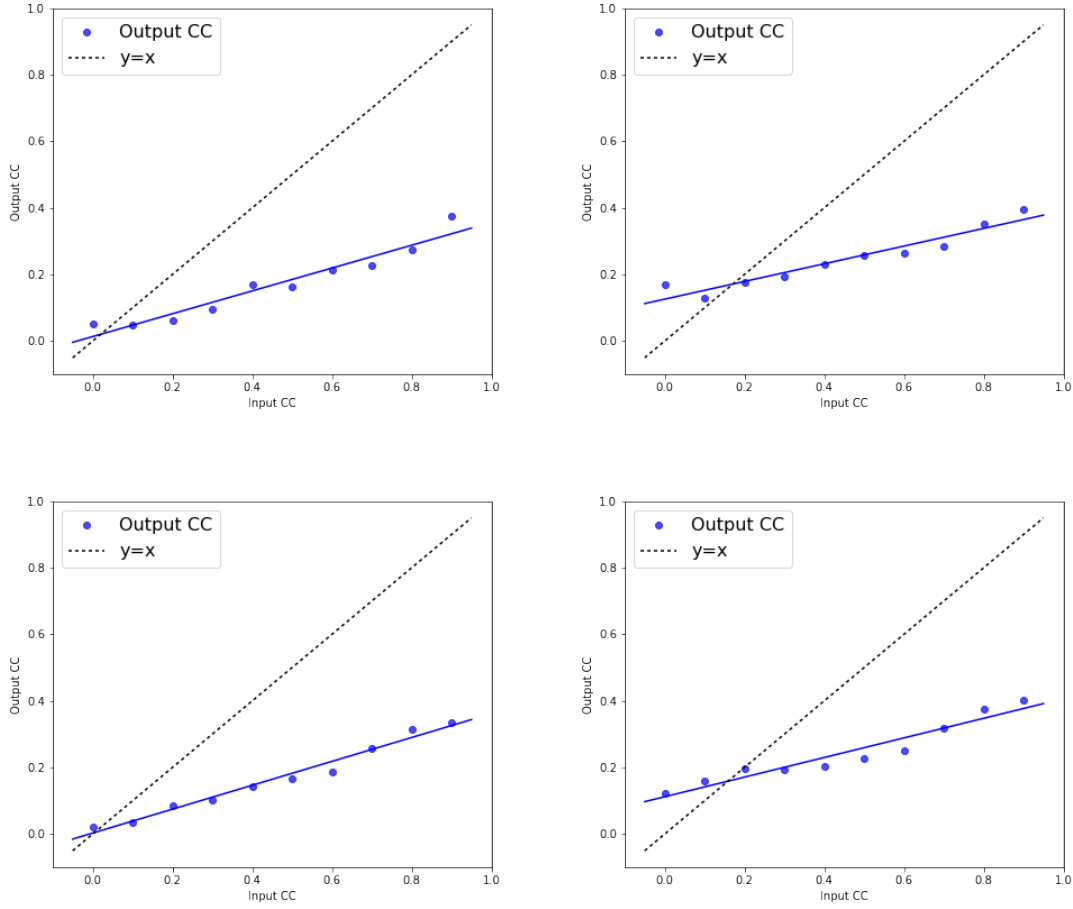


**Fig. 8.** [Color online] Input and output correlations for PD (first row from the top to the bottom) and healthy cell (second row). First column:  $\sigma_{\text{ref}} = 1$ . Right column:  $\sigma_{\text{ref}} = 4$ .

random refractory period in both healthy and PD cells leads to a linear increase in output correlations (see, for example, [9,28]).

Moreover, the presence of random inputs influences the spiking activity of STN neurons, both with and without deep brain stimulation (DBS) input currents. As the standard deviation of random refractory periods increases, the irregularity of spike trains decreases. Additionally, random refractory periods can mitigate the effects of random input currents in the system when DBS input currents are present. The interaction between random refractory periods and random input currents in STN cells with STDP membrane potential provides valuable insights for further model developments and progress in DBS therapy.

## 4 Conclusions

We introduced a modified HH model and outlined the process of synaptic conductance with random inputs and STDP. We highlighted the importance of the latter two factors in analyzing and managing neurodegenerative diseases, such as Parkinson's, in neuromorphic systems and other applications. By employing a Langevin stochastic dynamics framework in a numerical setting, we investigated the impact of random inputs on the membrane potential of STN cells. Specifically, we detailed the models used and provided numerical examples to examine the effects of random inputs on the time evolution of membrane potentials, neuronal spiking activities, and spike time irregularity profiles. Our results indicate that STDP enhances the regularity of

the ISI in spike trains of output neurons. However, the presence of a random refractory period, combined with random input currents, can significantly increase the irregularity of spike trains. Additionally, stochastic influences alongside STDP may enhance the correlation between neurons. These findings could offer insights into managing symptoms of Parkinson’s disease.

## Acknowledgment

Authors are grateful to the NSERC and the CRC Program for their support. RM is also acknowledging support of the BERC 2022-2025 program and Spanish Ministry of Science, Innovation and Universities through the Agencia Estatal de Investigacion (AEI) BCAM Severo Ochoa excellence accreditation SEV-2017-0718.

## References

1. A. A. Faisal and L. P. J. Selen and D. M. Wolpert: Noise in the nervous system. *Nature Reviews Neuroscience* 9, 292–303 (2008)
2. A. S. Powanwe and A. Longtin: Brain rhythm bursts are enhanced by multiplicative noise. *Chaos* 31, 013117 (2021)
3. Bujan, A.F., Aertsen, A., Kumar, A.: Role of input correlations in shaping the variability and noise correlations of evoked activity in the neocortex. *Journal of Neuroscience* 35(22), 8611–8625 (2015)
4. Chiken, S., Nambu, A.: Mechanism of deep brain stimulation: Inhibition, excitation, or disruption? *The Neuroscientist* 22(3), 313–322 (2016)
5. Christodoulou, C., Bugmann, G.: Coefficient of variation vs. mean interspike interval curves: What do they tell us about the brain? *Neurocomputing* 38–40, 1141–1149 (2001)
6. Cornelisse, L.N., Scheenen, W.J.J.M., Koopman, W.J.H., Roubos, E.W., Gielen, S.C.A.M.: Minimal model for intracellular calcium oscillations and electrical bursting in melanotrope cells of *xenopus laevis*. *Neural Computation* 13, 113–137 (2000)
7. David, F.J., Munoz, M.J., Corcos, D.M.: The effect of stn dbs on modulating brain oscillations: consequences for motor and cognitive behavior. *Experimental brain research* 238(7), 1659–1676 (2020)
8. Dayan, P., Abbott, L.F.: *Theoretical Neuroscience*. The MIT Press Cambridge, Massachusetts London, England (2005)
9. De La Rocha, J., Doiron, B., Shea-Brown, E., Josić, K., Reyes, A.: Correlation between neural spike trains increases with firing rate. *Nature* 448(7155), 802–806 (2007)
10. Dewell, R.B., Gabbiani, F.: Active membrane conductances and morphology of a collision detection neuron broaden its impedance profile and improve discrimination of input synchrony. *Journal of neurophysiology* 122(2), 691–706 (2019)
11. Dewell, R.B., Gabbiani, F.: Biophysics of object segmentation in a collision-detecting neuron. *eLife* 7, e34238 (2018)
12. Gallinaro, J.V., Clopath, C.: Memories in a network with excitatory and inhibitory plasticity are encoded in the spiking irregularity. *PLoS Comput Biol* 17(11), e1009593 (2021)
13. Gautam, A., Kohno, T.: An adaptive stdp learning rule for neuromorphic systems. *Frontiers in Neuroscience* 15, 741116 (2021)
14. Gautam, A., Kohno, T.: Adaptive stdp-based on-chip spike pattern detection. *Frontiers in Neuroscience* 17, 1203956 (2023)
15. Gerstner, W., Kistler, W.M., Naud, R., Paninski, L.: *Neuronal Dynamics: From single neurons to networks and models of cognition*. Cambridge University Press (2014)
16. Goupy, G., Tirilly, P., Bilasco, I.M.: Paired competing neurons improving stdp supervised local learning in spiking neural networks. *Frontiers in Neuroscience* 18, 1401690 (2024)
17. v. d. Groen, O., Mattingley, J.B., Wenderoth, N.: Altering brain dynamics with transcranial random noise stimulation. *Scientific Reports* 9(4029) (2019)
18. Gupta, A., Saurabh, S.: Unsupervised learning in a ternary snn using stdp. *IEEE Journal of the Electron Devices Society* (2024)
19. Herculano-Houzel, S.: Not all brains are made the same: new views on brain scaling in evolution. *Brain, behavior and evolution* 78(1), 22–36 (2011)
20. Hirschmann, J., Steina, A., Vesper, J., Florin, E., Schnitzler, A.: Neuronal oscillations predict deep brain stimulation outcome in parkinson’s disease. *Brain Stimulation* (2022)



21. Hong, S., Ratté, S., Prescott, S.A., De Schutter, E.: Single neuron firing properties impact correlation-based population coding. *Journal of Neuroscience* 32(4), 1413–1428 (2012)
22. Hussain, S.A., Sanki, P.K., et al.: Efficient in situ learning of hybrid lif neurons using wta mechanism for high-speed low-power neuromorphic systems. *Physica Scripta* 99(10), 106010 (2024)
23. Khoei, A.G., Javaheri, A., Kheradpisheh, S.R., Ganjtabesh, M.: Meta-learning in spiking neural networks with reward-modulated stdp. *Neurocomputing* 600, 128173 (2024)
24. Kim, S.Y., Lim, W.: Effect of interpopulation spike-timing-dependent plasticity on synchronized rhythms in neuronal networks with inhibitory and excitatory populations. *Cognitive Neurodynamics* 14(4), 535–567 (2020)
25. L. Zhang and Y. Zheng and J. Xie and L. Shi: Potassium channels and their emerging role in parkinson’s disease. *Brain Research Bulletin* 160, 1–7 (2020)
26. Lee, L.H.N., Huang, C.S., Wang, R.W., Lai, H.J., Chung, C.C., Yang, Y.C., Kuo, C.C.: Deep brain stimulation rectifies the noisy cortex and irresponsive subthalamus to improve parkinsonian locomotor activities. *npj Parkinson’s Disease* 8(1), 1–18 (2022)
27. Li, S., Liu, N., Yao, L., Zhang, X., Zhou, D., Cai, D.: Determination of effective synaptic conductances using somatic voltage clamp. *PLoS Comput Biol* 15(3), e1006871 (2019)
28. Liu, S., Wang, J., Fan, Y., Yi, G.: Effects of dendritic properties on spike train correlations in biophysically-based model neurons. *International Journal of Modern Physics B* 36(06), 2250061 (2022)
29. Lu, S., Sengupta, A.: Deep unsupervised learning using spike-timing-dependent plasticity. *Neuromorphic Computing and Engineering* 4(2), 024004 (2024)
30. Madadi Asl, M., Vahabie, A., Valizadeh, A., Tass, P.: Spike-timing-dependent plasticity mediated by dopamine and its role in parkinson’s disease pathophysiology. *Front. Netw. Physiol.* 2: 817524. doi: 10.3389/fnetp (2022)
31. Magee, J.C.: Observations on clustered synaptic plasticity and highly structured input patterns. *Neuron* 72(6), 887–888 (2011)
32. Ranganathan, G.N., Apostolides, P.F., Harnett, M.T., Xu, N.L., Druckmann, S., Magee, J.C.: Active dendritic integration and mixed neocortical network representations during an adaptive sensing behavior. *Nature neuroscience* 21(11), 1583–1590 (2018)
33. Roberts, J.A., Friston, K.J., Breakspear, M.: Clinical applications of stochastic dynamic models of the brain, part i: A primer. *Biological Psychiatry: Cognitive Neuroscience and Neuroimaging* 2, 216–224 (2017)
34. Rosa, M., Giannicola, G., Servello, D., Marceglia, S.R., Pacchetti, C., Porta, M., Sassi, M., Scelzo, E., Barbieri, S., Priori, A.: Subthalamic local field beta oscillations during ongoing deep brain stimulation in parkinson’s disease in hyperacute and chronic phases. *Neurosignals* 19, 151 – 162 (2011)
35. Shaheen, H., Melnik, R.: Deep brain stimulation with a computational model for the cortex-thalamus-basal-ganglia system and network dynamics of neurological disorders. *Computational and Mathematical Methods (Art.8998150)*, (2022), Art.8998150 (17 pages) (2022)
36. Sherf, N., Shamir, M.: Multiplexing rhythmic information by spike timing dependent plasticity. *PLoS computational biology* 16(6), e1008000 (2020)
37. So, R.Q., Kent, A.R., Grill, W.M.: Relative contributions of local cell and passing fiber activation and silencing to changes in thalamic fidelity during deep brain stimulation and lesioning: a computational modeling study. *J Comput Neurosci* 32, 499–519 (2012)
38. Stein, R.B., Gossen, E.R., Jones, K.E.: Neuronal variability: noise or part of the signal? *Nature Reviews Neuroscience* 6, 389–397 (2005)
39. T. K. T. Thieu, R. Melnik: Effects of random inputs and short-term synaptic plasticity in a LIF conductance model for working memory applications. In: Rojas, I., Valenzuela, O., Rojas, F., Herrera, L.J., Ortuño, F. (eds.) *Bioinformatics and Biomedical Engineering*. vol. 13346, pp. 59–72. Springer International Publishing, Cham (2022)
40. T. Zheng and K. Kotani and Y. Jimbo: Distinct effects of heterogeneity and noise on gamma oscillation in a model of neuronal network with different reversal potential. *Scientific Reports* 11(12960) (2021)
41. Tao, T., Li, D., Ma, H., Li, Y., Tan, S., Liu, E.x., Schutt-Aine, J., Li, E.P.: A new pre-conditioned stdp rule and its hardware implementation in neuromorphic crossbar array. *Neurocomputing* 557, 126682 (2023)
42. Teka, W., Marinov, T.M., Santamaria, F.: Neuronal spike timing adaptation described with a fractional leaky integrate-and-fire model. *PLoS Comput Biol* 10(3) (2014)
43. Thieu, T.K.T., Melnik, R.: Coupled effects of channels and synaptic dynamics in stochastic modelling of healthy and Parkinson’s-disease-affected brains. *AIMS Bioengineering* 9(2), 213–238 (2022)
44. Thieu, T.K.T., Melnik, R.: Effects of noise on leaky integrate-and-fire neuron models for neuromorphic computing applications. In: *Bioinformatics and Biomedical Engineering*. vol. 13375, pp. 3–18. Springer International Publishing, Cham (2022)
45. Traub, R.D., Wong, R.K., Miles, R., Michelson, H.: A model of CA3 hippocampal pyramidal neuron incorporating voltage-clamp data on intrinsic conductances. *J Neurophysiol* 66(2), 635–650 (1999)
46. Walters, B., Kalatehbali, H.R., Cai, Z., Genov, R., Amirsoleimani, A., Eshraghian, J., Azghadi, M.R.: Efficient sparse spiking auto-encoder for reconstruction, denoising and classification. *Neuromorphic Computing and Engineering* 4(3), 034005 (2024)

47. Wang, H., Dewell, R.B., Zhu, Y., Gabbiani, F.: Feedforward inhibition conveys time-varying stimulus information in a collision detection circuit. *Current Biology* 28(10), 1509–1521 (2018)
48. Wang, Y., Shi, X., Si, B., Cheng, B., Chen, J.: Synchronization and oscillation behaviors of excitatory and inhibitory populations with spike-timing-dependent plasticity. *Cognitive Neurodynamics* pp. 1–13 (2022)
49. X. Chen and B. Xue and J. Wang and H. Liu and L. Shi and J. Xie: Potassium channels: A potential therapeutic target for parkinson’s disease. *Neurosci. Bull.* 34(2), 341–348 (2018)
50. Y. C. Yang and C. H. Tai and M. K. Pan and C. C. Kuo: The T-type calcium channel as a new therapeutic target for Parkinson’s disease. *Pflugers Arch - Eur J Physiol* 446, 747–755 (2014)
51. Yamakou, M.E., Desroches, M., Rodrigues, S.: Synchronization in stdp-driven memristive neural networks with time-varying topology. *Journal of Biological Physics* 49(4), 483–507 (2023)